Radiometric Tests on Wet and Dry Antenna Reflector Surface Panels

T. Y. Otoshi and M. M. Franco
Ground Antenna and Facilities Engineering Section

The results of X-band noise temperature tests on two types of antenna surface panels are presented. The first type tested was a solid antenna panel, while the second type was a perforated panel with 3/16-in.-diameter holes. Measurements were made at 8.45 GHz using an X-band radiometric system.

Included in this article are measured noise temperature contributions from (1) thermal diffusive white paint on solid and perforated panels and (2) water sprayed on both painted and unpainted perforated panels. For this article, experiments on perforated panels were restricted to the 3/16-in.-diameter hole panels formerly used on Deep Space Network 64-m antennas. Rigorous calibration equations, applicable to a variety of antenna panel and dichroic plate test configurations, are presented. It has been demonstrated that an accurate, stable radiometric measurement system of the type used for the results of this article makes it possible to obtain information that would be much more difficult to obtain using other techniques.

I. Introduction

This article presents results of noise temperature measurements made at 8.45 GHz on (1) painted and unpainted, solid-aluminum sheet reflectors and (2) painted and unpainted, perforated panels having 3/16-in.-diameter holes. The results of recent noise temperature tests on a painted 1/8-in.-hole panel were reported by R. Stevens and R. Clauss.[1] Information concerning the dielectric constant and loss tangent of thermal diffusive white paint has been very difficult to obtain. To the authors' knowledge,

[1] R. Stevens and R. Clauss, "DSN Rain Effects Test Results and Recommendations," JPL Interoffice Memorandum RCC-89-019 (internal document), Jet Propulsion Laboratory, Pasadena, California, June 26, 1989.

the only other sources of experimental data on thermal diffusive white paint used on Deep Space Network (DSN) antennas are (1) a 1961 Dalmo-Victor report from which paint data were extracted and used in a 1971 report by Otoshi [1], and (2) an internal JPL report by A. Freiley,[2] who used an X-band cavity technique to obtain surface resistivity data.

Other radiometric measurements at 8.45 GHz on perforated panels have been made by S. Slobin and M. Franco in 1984.[3] They performed measurements on a number of *unpainted* perforated panels having different hole diameters. The panels were tested in both wet and dry conditions using a test setup and test procedures that were almost identical to those used to obtain the results of this article. The primary difference in the two test setups was that the Slobin/Franco setup used an X-band maser, while the setup for this article used an X-band high-electron-mobility transistor (HEMT).

In Section II the test method will be described. Rigorous calibration equations, applicable to a general class of panel and dichroic plate testing configurations, are also presented. Then radiometric test data will be presented and discussed. The data presented in this article will be useful for assessing whether or not paint on antenna panels is a problem at X-band.

II. Test Procedure

A. Measurement System Description

Noise temperature measurements were made with the radiometric system located on the roof of the Telecommunications building at the Jet Propulsion Laboratory (Building 238). In this test setup the X-band horn used is a 22-dB corrugated horn, and the low-noise amplifier is a cryogenically cooled X-band HEMT. The HEMT is followed by about 30 ft of phase-stable X-band coaxial cable, a post-amplifier, and a preselect filter which is terminated by a Hewlett Packard (HP) Model 436A power meter sensor. The preselector filter is tuned to a center frequency of 8.45 GHz ± 5 MHz. The test setup for this system was originally developed for purposes of measuring noise temperature increases due to rain on a DSN X-band dichroic plate.[4] When the horn is pointed at zenith sky, the operating noise temperature of the test setup at 8.45 GHz consists of the following noise temperature contributions:[5]

T_{cbr}	=	2.7 K	
T_{atm}	=	3.3 K	(clear sky, low humidity)
T_{horn}	=	1.5 K	
T_{wg}	=	3.0 K	
T_{hemt}	=	12.0 K	
T_{fup}	=	4.0 K	
T_{op}	=	26.5 K	

Above, T denotes noise temperature while the subscripts *cbr*, *atm*, *horn*, *wg*, *hemt*, *fup*, and *op*, respectively denote cosmic background radiation, atmosphere, horn, waveguide, HEMT, followup receiver, and operating. In this article, the terms operating noise temperature and system temperature will be used interchangeably.

Calibration of this measurement system is done with a Y-factor method described in [2] and performed automatically by computer control. Updated antenna operating noise temperatures are displayed on a monitor every 5 seconds. Details of the computer-controlled system are presented in Appendix A.

It was originally thought that the polarizer for the test setup was set for circular polarization, but was inadvertently set for elliptical polarization. The incorrect setting caused the measured results of the panel losses to be slightly higher than they would be for a circular polarization configuration. The equations that apply to the elliptical polarization configuration actually used are given in Appendix B.

B. Panel Measurement

The test configurations for the panel tests are shown in Fig. 1. All panels tested were 36 in. × 36 in. × 0.072 in. and located 36 in. from the horn aperture and held at an angle of 45 deg so that, with the horn horizontal to the ground, the angle of incidence is 45 deg for a plane wave signal radiated from zenith sky (Fig. 1). Measurements of operating noise temperatures were made at 8.45 GHz first with a solid aluminum reference plate held at 45 deg with respect to the horizon. Then the panel under test was placed at the same angle and the operating noise temperature was again measured. If all other noise temperatures remained constant during the test, subtraction of the two

[2] A. Freiley, "RF Evaluation of Paint Samples," JPL Interoffice Memorandum 3331-73-008 (internal document), Jet Propulsion Laboratory, Pasadena, California, March 9, 1973.

[3] S. D. Slobin and M. M. Franco, "X- and Ka-band Noise Temperature Effects from Wet Perforated Aluminum Panels Simulating Rain on DSN Antenna Surfaces," JPL Interoffice Memorandum 3331-84-003 (internal document), Jet Propulsion Laboratory, Pasadena, California, February 10, 1984.

[4] Stevens and Clauss, op. cit.

[5] M. Britcliffe, private communication.

measured operating noise temperatures will give the noise temperature difference between the panel under test and the reference plate.

To minimize measurement errors due to drift caused by changes in sky temperature versus time, the procedure used (to obtain the results for this article) was to take as many reference measurements as possible. A new reference measurement was taken after making measurements on two or three different test configurations.

The perforated panels were tested for the following three different "behind the panel" configurations: (1) horizon sky, (2) absorber, and (3) solid-aluminum plate.

For the perforated panel tests, the first test configuration (Fig. 1a) was to clamp the perforated panel to a wooden frame tilted at 45 deg. No additional reflecting plates or absorbers are placed behind the perforated panel. This test configuration is called the "horizon sky" behind-the-panel configuration because the signal that leaks through the panel will be absorbed primarily by the sky near the horizon. This configuration is convenient to use for quickly observing noise temperature differences. However, this setup is more susceptible to errors caused by changes in multiple reflections between fences, buildings, and other objects in close proximity to the test setup.

The second perforated panel test configuration was to place an absorber in back of the perforated panel to capture the leakage signal with an absorber at ambient temperature (see Fig. 1b). The difference between operating noise temperatures of this second configuration and that from the reference measurement provides information on leakage plus resistive panel losses of the perforated panel. For more details, refer to the equations presented in Appendix C.

The third configuration for testing perforated panels was to manually hold a solid-aluminum panel in back of the perforated panel at 45 deg with respect to level ground (see Fig. 1c). In this configuration, the signal that leaks through the perforated panel becomes reflected by the solid plate and becomes absorbed by zenith sky. As discussed in Appendix C, the difference between the operating noise temperature of this configuration and the reference measurement gives information on the resistive losses of the perforated panel.

Tests of wet test panels were made by spraying a fine mist of water on the panel. Due to the test panels being held at a 45-deg angle, most of the water ran off. Only some fine droplets and those retained due to surface tension over the holes stayed on the panel.

Rigorous calibration equations for the three different test configurations are presented in Appendix C. These equations are useful for understanding the calibrations procedure, the contributions from perforated plate leakage, and potential errors caused by unwanted spillover. It should be pointed out that if one is interested in determining specific dissipative loss contributions, it is not just a simple matter of subtracting two measured operating noise temperatures. It becomes necessary to examine all noise temperature components (associated with reflection, leakage, and dissipation) causing the operating noise temperature values to change. It is shown in Appendix C that if two nearly similar panels are being compared, so that reflected and leakage components are nearly the same for the two panels, then subtraction of the two operating noise temperatures will produce the desired dissipative loss noise temperature relative to that of the other plate being compared.

To experimentally determine how much power was actually spilling over the edges of the 36-in. × 36-in. test panel, a 24-in. × 24-in. absorber was moved around the perimeter of the test panel. An increased contribution of about 2.0 K was measured when the absorber was placed above the top edge of the panel. This measured increase is consistent with a theoretically calculated value obtained with theoretical near-field pattern and brightness temperature data. The near-field horn patterns were obtained for the X-band horn located 36 in. away from a 36-in. × 36-in. flat plate tilted at 45 deg. A separate report on this theoretical and experimental result is in preparation. As shown by the equations in Appendix C, the spillover loss does not affect the final test panel noise temperature values reported in this article, as long as the spillover-power to total-power ratio remains constant during measurement of the test plate and reference plate.

III. Experimental Results

The theoretical noise temperatures for an aluminum 6061 T6 solid panel (assuming a conductivity of 2.32×10^7 mhos/m) are 0.083 K and 0.165 K, respectively, for perpendicular and parallel polarizations for a 45-deg incidence angle at a frequency of 8.45 GHz. Then, for the elliptical polarization of the test setup (Appendix A), the theoretical effective noise temperature contribution due to this aluminum reference plate is calculated to be 0.153 K. If absolute values are of interest, the above calculated value can be applied to measurements that were made relative

to this reference plate. For this article, no corrections were made for the loss of the reference plate.

The measurements were started at 1:22 P.M. and completed at 2:04 P.M. on June 2, 1989. The total test time was 42 minutes and involved 29 different test configurations. In this test setup, the operating noise temperature value was displayed on a screen every 5 seconds. After a test configuration change was made, the values applicable to the test configuration of interest were written in a notebook. Table 1 shows the original recorded data, while Table 2 shows a tabulation of the reduced data. Table 1 may be useful as a guide for future test planning purposes. Table 2 shows the procedure for reducing the data from Table 1 for extracting particular noise temperature contributions of interest.

The information that can be extracted from the original data given in Table 1 are noise temperature increases due to (1) paint on a solid reflector, (2) paint on a perforated panel with 3/16-in.-diameter holes, (3) leakage through the holes of an unpainted perforated panel, (4) leakage through the holes of a painted perforated panel, (5) water spray on painted and unpainted perforated panels, (6) water spray on a painted solid panel, and (7) aluminum tape covering the holes of the unpainted perforated panel.

All test results apply only for test parameters with a 45-deg incidence angle, 8.45 GHz, and the elliptical polarization configuration described in Appendix A. Both the unpainted and painted perforated panels tested had 3/16-in.-diameter holes, 1/4-in. hole-to-hole spacings, equilateral triangle hole patterns, and a plate thickness of 0.072 in. The total thickness of the primer and Triangle Co. IR #6 thermal diffusive paint on the painted panels was measured with a micrometer and found to be about 0.002 in.

Although more data of interest exist in Table 2, an attempt will be made to summarize most of the highlights below:

(1) The increase of noise temperature due to paint on a solid-aluminum reflector was measured to be 0.1 K at 8.45 GHz for a 45-deg incidence angle. The repeatability of this measurement was ±0.1 K. See Table 2, item B1.

(2) The increase of noise temperature due to resistive losses for the unpainted perforated panel was 0.6 K. See Table 2, Item B2(c).

(3) The noise temperature component associated with perforated plate leakage was determined to be 0.8 K. See Table 2, Item B2(d). This measured value compares favorably with a theoretical value of 0.64 K calculated from Chen's Program [3] for the described perforated panel when the incidence angle is 45 deg and an elliptically polarized incident wave with 85.4 percent of the total power in the parallel polarization component and 14.6 percent in the perpendicular polarization component.

(4) The increase of noise temperature due to paint on the perforated panels with 3/16-in.-diameter holes was measured to be 0.2 K. See Table 2, Item B4(b). It is of interest to compare this value to the 0.1 K value that was measured for the paint contribution on a solid-aluminum plate (Table 2, Item B1).

(5) The increase of noise temperature due to water spray on an unpainted perforated panel with 3/16-in.-diameter holes was measured to be 11.6 K. See Table 2, Item B6(b). The measured value is about three times smaller than a theoretical value calculated for this panel when the holes are completely filled with water. During the measurement, it could be seen that the water layer only covered some of the holes near the panel surface and did not penetrate deeply into the holes. Most of the water began to drain off due to gravity, but water in some holes was retained because of surface tension.

(6) The increase of noise temperature due to water spray on a painted perforated panel with 3/16-in.-diameter holes was measured to be 7.3 K. See Table 2, Item B8(b). From comparisons with the 11.6 K value obtained for the unpainted perforated panel, it can be concluded that less water is retained by the painted panel than the unpainted panel.

(7) The increase of noise temperature due to water on a painted solid plate was measured to be 1.2 K. See Table 2, Item B11. Due to an oversight, no measurements were made of the noise temperature increase due to water sprayed onto the reference plate (the unpainted solid-aluminum plate).

IV. Discussion of Errors

It should be mentioned that the reported noise temperature contributions due to paint and water are larger than will be the case for a circularly polarized wave. The reason for this is that an unintentional error in the setting of the radiometric system polarizer caused about 85 percent of the power to be in the parallel polarization component and only 15 percent in the perpendicular polarization component. For a circularly polarized wave, the power is equally divided between the two polarization components. For the type of tests that were done on the two types of antenna reflector surface panels, a theoretical study shows that at a 45-deg incidence angle, the noise temperatures

for parallel polarization are significantly larger than those for perpendicular polarization.

The differential measurements involving paint contributions on the solid plate are believed to be accurate to within ±0.1 K. Errors due to drift (changing sky conditions) were small for the solid-plate measurements because the measurements were performed sequentially. For the perforated panel tests, there are several possible sources of errors in the reported data. Among these are uncorrectable operating system drifts due to changing sky conditions, an insufficiently large absorber for the absorber behind-the-perforated-panel tests, and an insufficiently large solid plate for the behind-the-panel test configuration. Water spray test data were difficult to repeat due to drainage and the uncontrollable amounts of water sprayed.

For a very accurate measurement of the resistive loss of a perforated panel, the solid plate in back of the perforated panel must be large enough to capture most (90 percent) of the leakage wave and be held at 45 deg, within ±5 deg. However, for the test setup used, the solid plate was only 36-in. × 36-in. and was held manually at an angle such that the solid plate was only approximately parallel to the perforated panel. The solid plate was only about 24 in. from the back side of the perforated panel (Fig. 1c). This distance was not large enough to keep multiple reflections from occurring between the solid panel and the back side of the perforated panel, but this fact was not known at the time of the measurements.

It is important to try to salvage the measured data concerning the resistive loss of the perforated plate because good experimental information concerning the resistive losses of perforated plates is very difficult to obtain. Resistive loss contributions in the past have been thought to be negligibly small and, therefore, seldom considered. For the perforated panel that was tested, the measured noise temperature contribution due to surface resistivity was 0.6 K with associated errors of about ±0.2 K. This result indicates that the resistive loss of a perforated panel is not as negligibly small as was previously assumed.

Slobin and Franco[6] have published experimental data that might be useful for determining the resistive losses of a number of perforated panels having different hole diameters. They used a larger (3 ft × 6 ft) solid-aluminum panel in back of the perforated panels at a sufficiently large distance so that the leakage signal did not undergo multiple bounces between the back side of the perforated panel and the solid plate. A study of the experimental data presented in Slobin and Franco's report supports the findings that the noise temperature contributions due to resistive losses of unpainted perforated panels are much larger than previously believed. Theoretical values for resistive losses of perforated plates were calculated in the past through the use of a simple formula derived by Otoshi [4]. The previous formula now appears to be incorrect. As a result of recent experimental discoveries, a new formula has been derived for calculating perforated panel resistive losses. The validity of this new formula is currently being investigated and will be reported on separately.

V. Recommendations for Future Tests

The procedure to minimize errors due to sky noise temperature changes was to make as many reference measurements as might be practical. Then, differences were taken between the operating noise temperature of the configuration under test and the operating noise temperature of the nearest (in time) reference plate measurement. An improved procedure would have been to record the test times (hr, min) for each configuration, including the reference readings. Then, interpolation between reference plate readings could have been used to obtain a reference value that corresponded to the mid-time that measurements were made for the test configuration of interest. In this manner, the errors due to drift could have been reduced to a negligibly small value.

Figure 2 shows the magnitude of the drift relative to the operating noise temperature measured for all test configurations. The reference measurement drift is shown more clearly on a magnified scale in Fig. 3. The total drift in the reference operating noise temperature was 0.5 K in about 40 minutes of time. Had the actual test times of the configurations been recorded, then correction could have been made for the drift. Many reference readings were taken because thin clouds occasionally drifted over the main beam of the horn. For interest, the data points for the painted solid-plate measurements are also shown in Fig. 3. It can be seen that measurements on the painted solid-plate were done immediately after measurements on the reference plate. Therefore, drift error was minimal for determining the noise contributions of paint on the solid plate.

It should be mentioned that if one is interested in a particular noise temperature contribution such as paint on perforated panels, better test procedures than the ones described in this article could be developed. For example, if it had been the primary objective to determine the noise temperature contributions due to paint on a perfo-

[6] Slobin and Franco, op. cit.

rated panel, then measurements of unpainted and painted perforated panels should be made sequentially rather than being taken relative to the reference plate.

A future improvement to the current computer-aided measurement system might be to have a computer program where the experimentor can type in a data file name, test configuration title, and the number of data points to be recorded. The computer then opens the specified data file and records the information into the data file and provides a prompt for start of the test. After the return key is hit, the specified number of operating noise temperature data points is measured. The computer averages the data, computes a standard deviation, records the computed data, records the mid-test time, and then closes the file. This feature would free the experimentor from having to rapidly write down numbers and avoid possible transcribing errors.

From the experience gained from these tests, it was found beneficial to have two people involved in performing the tests. One person is needed to devote full time to making configuration changes and preparing for the next change, while the second person is needed to write down the measured values. Speed is of the essence if the sky noise temperature is changing significantly such as would be caused by clouds drifting overhead.

VI. Concluding Remarks

A large amount of very useful data concerning paint contributions on solid and perforated panels have been obtained. In addition, new information was obtained on the resistive losses of perforated plates at X-band. The fact that reliable and repeatable data were obtained on 29 configurations (see Table 1) in about 40 minutes time is a tribute to the general usefulness of the noise temperature measurement system for performing these types of tests.

It has been demonstrated that an accurate, stable radiometric measurement system of the type used for the results of this article makes it possible to obtain information that would be much more difficult to obtain using other techniques. For example, the contributions of paint and resistive losses of perforated panels were easy to measure with the radiometric system that was used. A waveguide technique to determine perforated plate resistive losses requires ultraprecision and specially imaged waveguide samples [4]. Resistive loss on perforated panels cannot be determined with the cavity technique[7] because the loss due to leakage through the perforated holes cannot be isolated from the loss due to surface resistivity.

[7] Freiley, op. cit.

Acknowledgments

M. Britcliffe of the Radio Frequency and Microwave Subsystems Section (Section 333) developed the radiometric measurement system described in this article and gave permission to use the test setup for making the panel measurements. All panels for the noise temperature tests were furnished by V. Lobb of the Ground Antenna and Facilities Engineering Section.

References

[1] T. Y. Otoshi, "Antenna Noise Temperature Contributions due to Ohmic and Leakage Losses of the DSS 14 64-m Antenna Reflector Surface," *DSN Progress Report for July and August 1971,* Technical Report 32–1526, vol. 26, no. V, pp. 115–119, Jet Propulsion Laboratory, Pasadena, California, October 15, 1971.

[2] C. T. Stelzried, "Operating Noise Temperature Calibrations of Low Noise Receiving Systems," *Microwave Journal,* vol. 14, no. 6, pp. 41–48, June 1971.

[3] C. C. Chen, "Transmission of Microwave Through Perforated Plates of Finite Thickness," *IEEE Transactions on Microwave Theory and Techniques,* vol. MTT-21, pp. 1–6, January 1973.

[4] T. Y. Otoshi, "Precision Reflectivity Loss Measurements of Perforated Plate Mesh Materials by a Waveguide Technique," *IEEE Transactions on Instrumentation and Measurements (Special Issue),* vol. IM–21, no. 4, pp. 451–457, November 1972.

Table 1. Original data

Test. No.	Test Configuration	Readings of T_{op}, K	Average T_{op}, K	Comments
A1	Unpainted solid-aluminum sheet (unclean side)	27.00, 26.99 26.99	26.99	
A2	Reference reading unpainted aluminum sheet (clean side)	26.93, 26.87 26.85, 26.54 26.55, 26.60	26.72	Turned sheet to other side and wiped
A3	Painted solid-aluminum sheet	26.93, 26.97 26.95	26.95	Test A3–Test A2 values give paint loss
A4	Unpainted 3/16-in.-diameter hole panel, dry, horizon sky behind panel	27.63, 27.64 27.63	27.63	
A5	Unpainted 3/16-in.-diameter hole panel, dry, absorber behind panel	27.98, 27.99 28.00, 27.99	27.99	Test A5–Test A7 values give perforated panel dissipation and leakage loss
A6	Unpainted 3/16-in.-diameter hole panel, dry, solid plate behind panel	27.24, 27.25 27.23	27.24	
A7	Reference reading unpainted aluminum sheet (clean side)	26.67, 26.65 26.64	26.65	Compare to Test A2 reference value of 26.72 K
A8	Painted solid-aluminum sheet	26.81, 26.77 26.72, 26.77	26.78	Test A8–Test A7 values give paint loss
A9	Painted 3/16-in.-diameter hole panel, dry, horizon sky behind panel	27.75, 27.75 27.75	27.75	
A10	Painted 3/16-in.-diameter hole panel, dry, absorber behind panel	28.16, 28.19 28.18	28.18	Compare to Test A5 results
A11	Painted 3/16-in.-diameter hole panel, dry, solid plate behind panel	27.50, 27.52 27.48	27.50	
A12	Reference reading unpainted aluminum sheet (clean side)	26.61, 26.61 26.57	26.60	Compare to Test A7 reference value of 26.65 K
A13	Painted solid-aluminum sheet	26.77, 26.77 26.70	26.73	Test A13–Test A12 values give paint loss
A14	Unpainted 3/16-in.-diameter hole panel, wet, horizon sky behind panel	43.30, 41.70 41.09	42.04	Water draining off during test
A15	Unpainted 3/16-in.-diameter hole panel, wet, absorber behind panel	39.48, 39.26	39.37	Water draining off during test
A16	Unpainted 3/16-in.-diameter hole panel, wet, solid plate behind panel	38.60, 38.40 38.30	38.43	Water draining off during test
A17	Same as Test A16 except more water sprayed on panel, solid plate behind panel	40.97, 43.30 40.42	41.56	
A18	Reference reading unpainted aluminum sheet (clean side)	26.44, 26.42 26.43	26.43	Compare to Test A12 reference value of 26.60 K

Table 1 (contd)

Test. No.	Test Configuration	Readings of T_{op}, K	Average T_{op}, K	Comments
A19	Painted solid-aluminum sheet	26.57, 26.58 26.59	26.58	Test A19–Test A18 values give paint loss
A20	Painted 3/16-in.-diameter hole panel, wet, horizon sky behind panel	35.37, 36.18 35.60	35.72	Water draining off during test
A21	Painted 3/16-in.-diameter hole panel, wet, absorber behind panel	35.40, 35.37 35.25	35.34	Water draining off during test
A22	Painted 3/16-in.-diameter hole panel, wet, solid plate behind panel	34.97, 35.02 35.04	35.01	Water draining off during test
A23	Reference reading unpainted aluminum sheet (clean side)	26.42, 26.37 26.37	26.39	Compare to Test A18 reference value of 26.43 K
A24	Painted solid-aluminum sheet	26.49, 26.48 26.47	26.48	Test A24–Test A23 values give paint loss
A25	Painted solid-aluminum sheet, wet	30.17, 26.98 26.70, 26.67	27.63	Test A25–Test A24 values give water film loss on painted aluminum sheet
A26	Unpainted 3/16-in.-diameter hole panel, covered with 2-in.-wide aluminum tape (not too carefully done). Plate was not clamped to be as flat as in Test A4.	29.71, 29.74 29.71	29.72	Test A26–Test A28 values give aluminum tape loss (inconclusive)
A27	Same as Test A26 except wet	32.49, 35.89 30.94, 31.30	32.66	
A28	Reference reading unpainted aluminum sheet (clean side)	26.23, 26.21 26.22, 26.21	26.22	Compare to Test A23 reference value of 26.39 K
A29	Painted solid-aluminum sheet (dried out)	26.23, 26.25 26.24	26.24	Test A29–Test A28 values give paint loss

Table 2. Reduced test data from original data in Table 1

Item Id.	Item Being Tested and Test Configuration	Noise Temperature Contribution, K	Average K	Comments
B1	Increase due to white paint only on 6061 T6 aluminum sheet	(A# values are given in Table 1) A3 − A2 = 0.23 A8 − A7 = 0.13 A13 − A12 = 0.13 A19 − A18 = 0.15 A24 − A23 = 0.09 A29 − A28 = 0.02	0.1	Repeatability is ± 0.1 K
B2	Dry unpainted aluminum antenna panel with 3/16-in.-diameter holes			
	(a) With horizon sky behind panel	(from Table 1) 27.63 − 26.72 = 0.91 A4 A2	0.9	
	(b) With absorber behind panel	27.99 − 26.65 = 1.34 A5 A7	1.3	Approximate NT due to resistive and leakage losses
	(c) With solid plate behind panel	27.24 − 26.65 = 0.59 A6 A7	0.6	Approximate resistive loss NT for unpainted perforated panel
	(d) Calculations	(from this Table) 1.34 − 0.59 = 0.75 B2(b) B2(c)	0.8	Approximate NT due to leakage
B3	Dry painted aluminum antenna panel with 3/16-in.-diameter holes			
	(a) Horizon sky	(from Table 1) 27.75 − 26.65 = 1.10 A9 A7	1.1	
	(b) Absorber	28.18 − 26.60 = 1.58 A10 A12	1.6	Approximate NT due to resistive and leakage losses
	(c) Solid plate	27.50 − 26.60 = 0.90 A11 A12	0.9	Approximate NT due to resistive loss only
	(d) Calculations	(from this Table) 1.58 − 0.90 = 0.68 B3(b) B3(c)	0.7	Approximate NT due to leakage loss only
B4	Noise temperature increase due only to white paint on dry aluminum panels with 3/16-in.-diameter holes. Calculations based on unpainted and painted panel data with the same configurations behind the panels. It is interesting to compare the following results to the 0.13-K value for the painted solid panel.			
	(a) Horizon sky	(from this Table) 1.10 − 0.91 = 0.19 B3(a) B2(a)	0.2	Sensitive to changes in low elevation-angle sky temperature
	(b) Absorber	1.58 − 1.34 = 0.24 B3(b) B2(b)	0.2	Most accurate result
	(c) Solid plate	0.90 − 0.59 = 0.31 B3(c) B2(c)	0.3	Difficult to accurately position the solid plate

Table 2 (contd)

Item Id.	Item Being Tested and Test Configuration	Noise Temperature Contribution, K	Average K	Comments
B5	Unpainted aluminum antenna panel with 3/16-in.-diameter holes in wet condition after water sprayed on front side			
	(a) Horizon sky	(from Table 1) 42.04 − 26.60 = 15.44 A14 A12	15.4	
	(b) Absorber	39.37 − 26.43 = 12.94 A15 A18	12.9	Approximate resistive and leakage loss NT
	(c) Solid plate	38.43 − 26.43 = 12.00 A16 A18	12.0	Approximate resistive loss NT
	(d) Solid plate after more water sprayed	41.56 − 26.43 = 15.13 A17 A18	15.1	Approximate resistive loss NT
	(e) Calculations	(from this Table) 12.9 − 12.0 = 0.90 B5(b) B5(c)	0.9	Approximate leakage loss NT for wet panel
B6	Noise temperature increase due to water on *unpainted* aluminum panel with 3/16-in.-diameter holes			
	(a) Horizon sky	(from this Table) 15.44 − 0.91 = 14.53 B5(a) B2(a)	14.5	
	(b) Absorber	12.94 − 1.34 = 11.60 B5(b) B2(b)	11.6	
	(c) Solid plate	12.00 − 0.59 = 11.41 B5(c) B2(c)	11.4	
	(d) Solid plate after more water sprayed	15.13 − 0.59 = 14.54 B5(d) B2(c)	14.5	
B7	Painted aluminum antenna panel with 3/16-in.-diameter holes in wet condition after water sprayed on front side			
	(a) Horizon sky	(from Table 1) 35.72 − 26.43 = 9.29 A20 A18	9.3	
	(b) Absorber	35.34 − 26.43 = 8.91 A21 A18	8.9	Approximate resistive and leakage loss NT
	(c) Solid plate	35.01 − 26.39 = 8.62 A22 A23	8.6	Approximate resistive loss NT
	(a) Calculations	(from this Table) 8.91 − 8.62 = 0.29 B7(b) B7(c)	0.3	Approximate leakage loss NT
B8	Noise temperature increase due to water on *painted* aluminum antenna panel with 3/16-in.-diameter holes			
	(a) Horizon sky	(from this Table) 9.29 − 1.10 = 8.19 B7(a) B3(a)	8.2	
	(b) Absorber	8.91 − 1.58 = 7.33 B7(b) B3(b)	7.3	Water draining
	(c) Solid plate	8.62 − 0.90 = 7.72 B7(c) B3(c)	7.7	

Table 2 (contd)

Item Id.	Item Being Tested and Test Configuration	Noise Temperature Contribution, K	Average K	Comments
B9	Differences of noise temperature increase due to water on *unpainted* and *painted* aluminum panel with 3/16-in.-diameter hole			
	(a) Horizon sky	(from this Table) 15.44 − 9.29 = 6.15 B5(a) B7(a)	6.2	
	(b) Absorber	12.94 − 8.91 = 4.03 B5(b) B7(b)	4.0	Water draining off
	(c) Solid plate	12.00 − 8.62 = 3.38 B5(c) B7(c)	3.4	
	Note: For all of the above test configurations, the unpainted panel with water has a higher noise temperature than the painted panel with water.			
B10	Water sprayed on white painted solid 6061 T6 aluminum sheet	(from Table 1) 27.63 − 26.39 = 1.24 A25 A23	1.2	Relative to the reference plate
B11	Increase due only to water sprayed on white painted solid 6061 T6 aluminum sheet	(from this Table) 1.24 − 0.13 = 1.11 B10 B1	1.1	
		(from Table 1) 27.63 − 26.48 = 1.15 A25 A24	1.2	This value is more accurate
B12	Aluminum-tape-covered unpainted aluminum antenna panel with 3/16-in.-diameter holes	(from Table 1) 29.72 − 26.22 = 3.50 A26 A28	3.5	Taped panel not clamped well to test frame
B13	Water sprayed on aluminum-tape-covered antenna panel with 3/16-in.-diameter holes	(from Table 1) 32.66 − 26.22 = 6.44 A27 A28	6.4	
B14	Increase due only to water sprayed on aluminum-tape-covered antenna panel with 3/16-in.-diameter holes	(from this Table) 6.44 − 3.50 = 2.94 B13 B12	2.9	

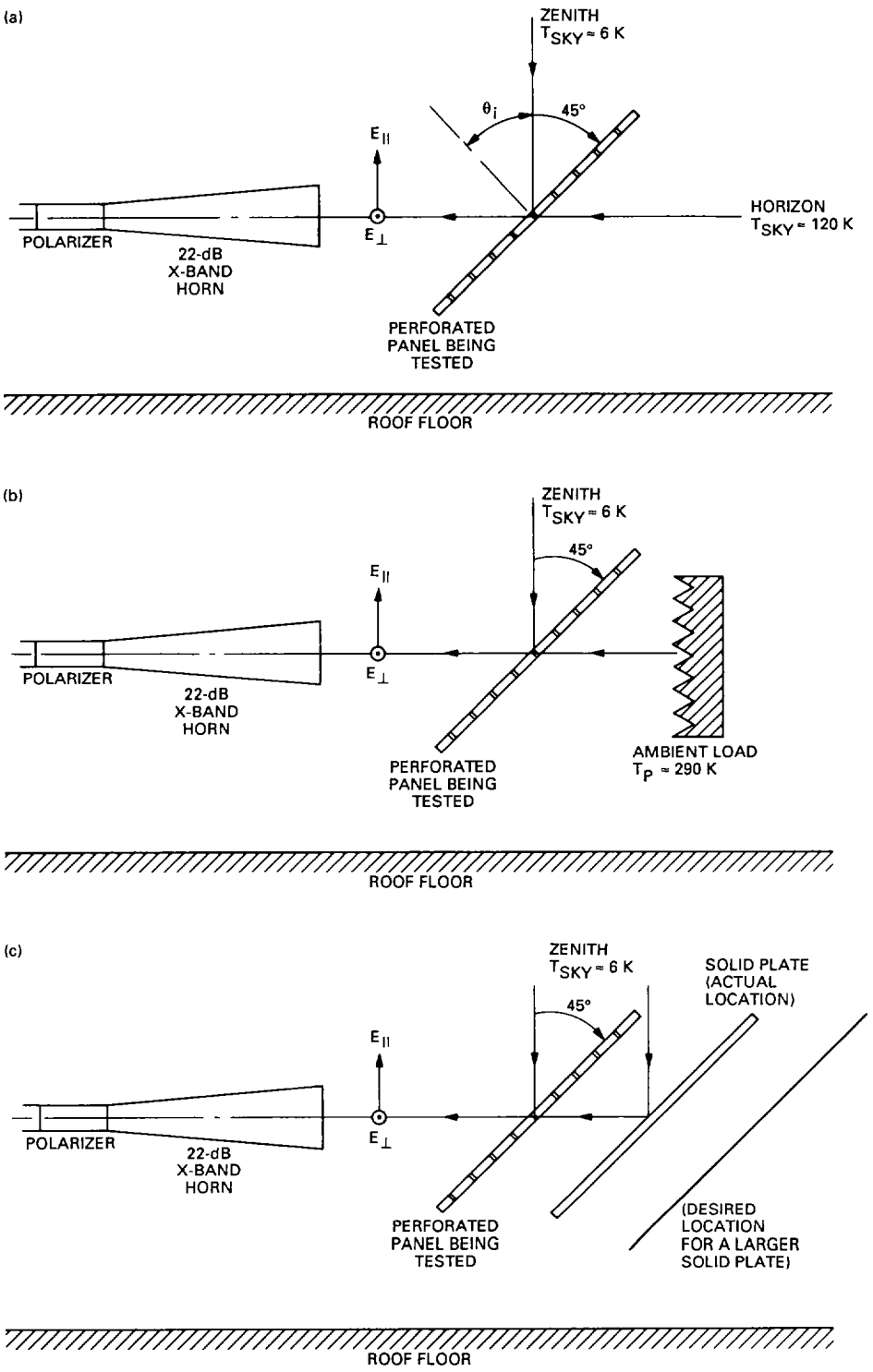

Fig. 1. Radiometric test setup showing the: (a) horizon sky, (b) absorber, and (c) solid plate behind-the-panel test configurations.

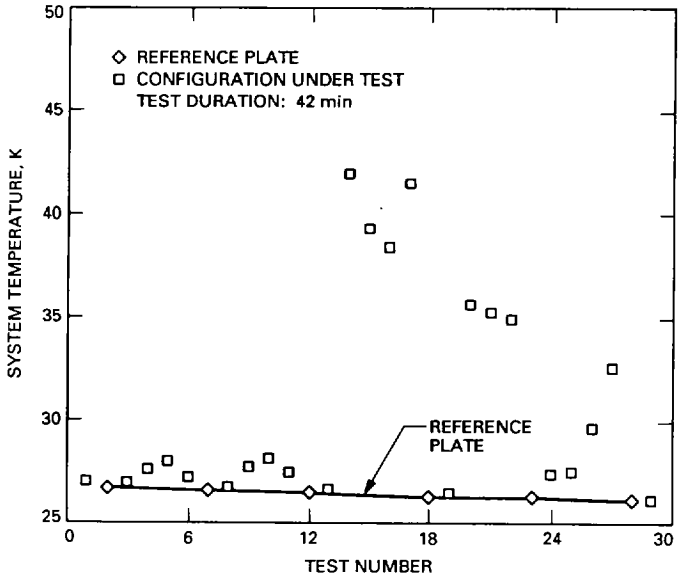

Fig. 2. Measured operating (system) noise temperatures versus test number. Descriptions of the tests are given in Table 1.

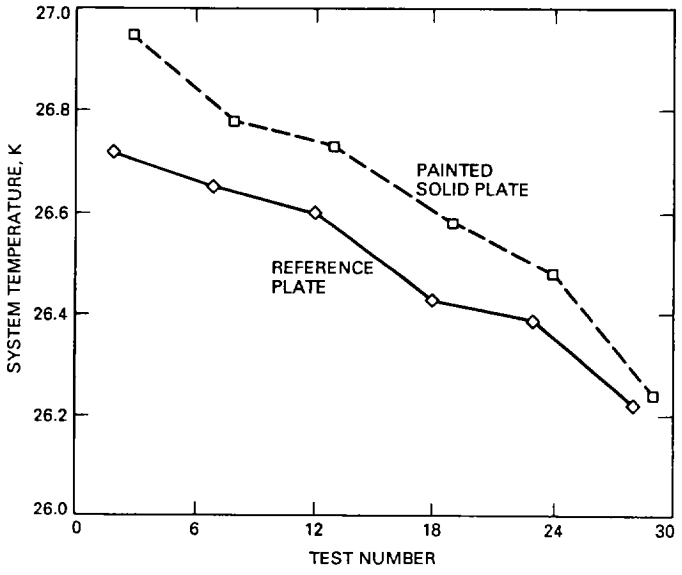

Fig. 3. Measured operating noise temperatures for the unpainted and painted solid-aluminum plate reflectors. The unpainted plate was used for all reference measurements.

Appendix A

Computer-Controlled Operating Noise Temperature Measurement System

A brief description of the special automatic features of the test setup will be given in this Appendix. For the test setup decribed in this article, it was not required that an aperture ambient load be placed over the horn in order to make Y-factor measurements for measuring the operating noise temperature. Instead the ambient load for this test setup is a waveguide load connected to a remote controllable waveguide switch.

In this automatic measurement system, a computer first commands the waveguide switch to switch to the "ambient load" position so that the waveguide ambient load is connected to the input to the HEMT. The ambient load physical temperature, furnished by a digital thermometer, is read by the computer. A command is then sent to rezero the HP digital power meter. Then, for a duration of about 5 sec, the average received power in the "ambient load" configuration is measured with the HP digital power meter and read by the computer.

The computer then commands the waveguide switch to switch to the "horn" position so that the horn is connected to the input of the HEMT. A measurement of the average received noise power in the "horn" position is then measured with the HP power meter for about 5 sec. Then, from the two measured noise power values (ambient load and horn) and a Y-factor equation [2], the operating noise temperature for the horn system configuration is computed and displayed on the computer monitor. Then, the average received noise power for the horn configuration is again measured for 5 sec. The noise power measured previously for the ambient load configuration is assumed to be constant and used again to compute a new operating noise temperature for the current horn configuration. A new value of antenna operating noise temperature is obtained every 5 sec and displayed on the computer monitor.

After 15 min, the computer commands the waveguide switch to return to the "ambient load" position and the entire sequence is repeated. This procedure results in the system being recalibrated every 15 min. The assumption is made that the ambient load and receiver noise temperatures do not change during the 15-min period between calibration and recalibration. The assumption is a good one, provided that the ambient load temperature does not change more than about ± 3 K over the 15-min test period. The other assumption, that the receiver noise temperature be constant, is a good one because tests have shown that the HEMT noise temperature does not change more than ± 0.2 K over long periods (12 hr) of time. Test results from DSS 13 indicate that the X-band HEMT stability is also insensitive to changes in physical orientation (elevation angle).

Appendix B

Noise Temperature for Elliptical Polarization Configuration

Although it was originally thought that the polarizer for the test setup was set for circular polarization, it was found that installed polarizer was inadvertently set to 22.5 deg rather than 45 deg with respect to the E-field orientation of the rectangular waveguide. Thus, for the actual elliptical polarization configurations that existed for the tests, the following equations apply:

$$\left[\frac{\text{parallel pol. power}}{\text{total power}}\right] = \cos(22.5)\cos(22.5) = 0.854$$

$$\left[\frac{\text{perp. pol. power}}{\text{total power}}\right] = \sin(22.5)\sin(22.5) = 0.146$$

The measured noise temperature (NT) is then

$$NT = 0.854(NT)_{\|} + 0.146(NT)_{\perp}$$

where $(NT)_{\|}$ and $(NT)_{\perp}$ are the noise temperatures of the antenna panel that would be measured if the polarizer was set for receiving only parallel and perpendicular polarizations, respectively.

Appendix C

Noise Temperature Equations for Various Test Configurations

A. Operating Noise Temperature

For the test setups shown in Fig. 1, a general expression for the antenna system operating noise temperature is

$$T_{opa} = T_a + T_r \tag{C-1}$$

where T_a is the antenna noise temperature defined at the horn aperture and T_r is the receiver effective noise temperature defined at the horn aperture. The units are in kelvins.

The receiver consists of the horn, waveguide (polarizer, transition, and switch) connecting the horn to the HEMT, the HEMT, and the followup receiver. For purposes of this article, the receiver noise temperature is assumed to be constant and only the antenna noise temperature changes with the test configuration. Therefore, only expressions of T_a for the different test configurations will be provided.

B. Solid-Plate Test Configuration

Let $T_{a,sp}$ be the antenna noise temperature for the test configuration that involves the use of the solid aluminum plate test as the reference. Furthermore, let $T_{a',sp}$ be the general symbol for antenna noise temperature when the plate has a layer of paint or water. Then, if the solid plate replaces the perforated plate shown in the test setup of Fig. 1(a), it can be seen that

$$T_{a,sp} = A_{sp}\left[|(S11)_{sp}|^2 T_{sky,zen} + D_{sp}T_p\right] + (1 - A_{sp})\,T_{b,sp} \tag{C-2}$$

$$T_{a',sp} = A'_{sp}\left[|(S11')_{sp}|^2\, T_{sky,zen} + D'_{sp}T_p\right] + \left(1 - A'_{sp}\right)T_{b',sp} \tag{C-3}$$

where the A_{sp} is the fraction of total power captured by the solid reference plate, $T_{b,sp}$ is the average brightness temperature as seen by the spillover (uncaptured) power, and $|(S11)_{sp}|^2$ and D_{sp} are, respectively, the fractions of total incident power that are reflected and dissipated by the reference plate. The primed symbols have the same definitions as the corresponding unprimed symbols except that they apply to the solid plate having the paint or water layer. The symbol $T_{sky,zen}$ is the brightness temperature as seen looking at the sky in the zenith direction and consists of noise contributions due to the atmosphere, cosmic background radiation, and the galaxy; T_p is the physical (or ambient) temperature in kelvins. It is assumed that the physical temperatures of the painted and unpainted (or wet) plates are the same during the test.

In Eqs. (C-2) and (C-3), it is of interest to note from conservation of energy considerations that

$$D_{sp} = 1 - |(S11)_{sp}|^2$$

$$D'_{sp} = 1 - |(S11')_{sp}|^2$$

and $|(S11)_{sp}|^2$ and $|(S11')_{sp}|^2$ can never be equal to unity in practice because of finite metal surface resistivity of the solid plate. Assuming that the spillover power ratio is the same in the two test configurations (i.e., $A'_{sp} = A_{sp}$), and $T_{b,sp} = T_{b;sp}$ then subtraction of the operating noise temperatures, using Eqs. (C-1), (C-2), and (C-3), leads to the result

$$T_{a',sp} - T_{a,sp} = A_{sp}\left[|(S11')_{sp}|^2 - |(S11)_{sp}|^2\right] T_{sky,zen} + \left(D'_{sp} - D_{sp}\right) T_p \tag{C-4}$$

For the solid plate with paint

$$|(S11')_{sp}|^2 \simeq |(S11)_{sp}|^2$$

and since for this test setup used at X-band, $T_{sky,zen} =$ 6 K, the first term in Eq. (C-4) becomes very small compared to the other terms and may be dropped. A theoretical study showed that the same assumption can be made for the case of a thin layer of water on a solid reflector surface. Then it can be seen from Eq. (C-4) that subtraction of the two operating noise temperatures will lead to the differential noise temperature increase due to dissipative loss of the paint or water.

To account for polarization then, in Eqs. (C-2) and (C-3) one needs only to substitute the expressions

$$|(S11)_{sp}|^2 = |(S11)_{sp,\|}|^2 \cos^2\theta_p + |(S11)_{sp,\perp}|^2 \sin^2\theta p \tag{C-5}$$

$$|(S11')_{sp}|^2 = |(S11')_{sp,\|}|^2 \cos^2\theta_p + |(S11')_{sp,\perp}|^2 \sin^2\theta p \tag{C-6}$$

where $|(S11)_{sp,\|}|^2$ and $|(S11)_{sp,\perp}|^2$ are, respectively, the power reflection coefficient for parallel and perpendicular polarizations for the reference plate and primed symbols apply to the test plate configuration. The symbol θ_p is the polarizer angle defined such that when $\theta_p = 0$, all of the reflected power is in the parallel polarization component.

C. Perforated Panel in the Horizon Sky Behind-the-Panel Configuration

For the horizon sky behind-the-panel configuration shown in Fig. 1(a), let $T_{a,pp,hor}$ and $T_{a',pp,hor}$ be defined as the antenna noise temperatures, respectively, for the unpainted and painted (or wet) perforated panel test configurations. Then, from Fig. 1(a), it can be seen that

$$T_{a,pp,hor} = A_{pp}[|(S11)_{pp}|^2\, T_{sky,zen} + D_{pp}T_p + |(S21)_{pp}|^2 T_{sky,hor}] + (1 - A_{pp})\, T_{b,pp} \tag{C-7}$$

$$T_{a',pp,hor} = A'_{pp}[|(S11')_{pp}|^2\, T_{sky,zen} + D'_{pp}T_p + |(S21')_{pp}|^2 T_{sky,hor}] + (1 - A'_{pp})\, T_{b',pp} \tag{C-8}$$

where A_{pp} is the fraction of total power captured by the unpainted perforated reference plate and $T_{b,pp}$ is the average brightness temperature as seen by the spillover (uncaptured) power. The symbols $|(S11)_{pp}|^2$, $|(S21)_{pp}|^2$, and D_{pp} are, respectively, the fractions of total incident power reflected, transmitted, and dissipated by the unpainted perforated plate. The primed symbols have the same definitions as the corresponding unprimed symbols except that they apply to the perforated plate having a layer of paint or water. The symbol $T_{sky,hor}$ is the brightness temperature as seen looking at the sky in the horizon direction.

From conservation of energy considerations, in Eqs. (C-6) and (C-7), we could have let

$$D_{pp} = 1 - |(S11)_{pp}|^2 - |(S21)_{pp}|^2$$

$$D'_{pp} = 1 - |(S11')_{pp}|^2 - |(S21')_{pp}|^2$$

but it is clearer to explicitly show the dissipative components of interest as was done previously.

When the operating noise temperatures for the primed and unprimed expressions are differenced for this test configuration, this corresponds to subtracting Eq. (C-7) from (C-8). For most perforated panel testing, the differential term involving $T_{sky,zen}$ is typically small compared to other terms and, therefore, can be dropped. The end result will be an expression for the differential noise contribution due to dissipation except for an error term involving $T_{sky,hor}$, which can also be neglected if the difference in leakage wave contributions for the two cases is small. The differential leakage wave contribution will be small if

$$|(S21')_{pp}|^2 - |(S21)_{pp}|^2 \approx 0$$

The above assumption may be valid for the tests involving comparisons of painted and unpainted panels, but not necessarily valid for tests involving comparisons of wet and dry panels.

Differencing the above primed and unprimed antenna temperatures, for the wet and dry panel tests, will give a net change due to changes in reflection, dissipation, and leakage. The measured change would still be of interest, but it cannot be stated that the entire change was caused by differences in dissipative loss alone.

For tests on the perforated panels, the polarization can be accounted for by substitutions of the following expressions into Eqs. (C-7) and (C-8):

$$|(S11)_{pp}|^2 = |(S11)_{pp,\|}|^2 \cos^2\theta_p + |(S11)_{pp,\perp}|^2 \sin^2\theta_p \tag{C-9}$$

$$|(S21)_{pp}|^2 = |(S21)_{pp,\|}|^2 \cos^2\theta_p + |(S21)_{pp,\perp}|^2 \sin^2\theta_p \tag{C-10}$$

$$|(S11')_{pp}|^2 = |(S11')_{pp,\|}|^2 \cos^2\theta_p + |(S11')_{pp,\perp}|^2 \sin^2\theta_p \tag{C-11}$$

$$|(S21')_{pp}|^2 = |(S21')_{pp,\|}|^2 \cos^2\theta_p + |(S21')_{pp,\perp}|^2 \sin^2\theta_p \tag{C-12}$$

where $|(S11)_{pp,\|}|^2$ and $|(S11)_{pp,\perp}|^2$ are, respectively, the power reflection coefficients of the unpainted perforated panels for parallel and perpendicular polarizations. Then, $|(S21)_{pp,\|}|^2$ and $|(S21)_{pp,\perp}|^2$ are, respectively, the power transmission coefficients of the unpainted perforated panels for parallel and perpendicular polarizations. The primed symbols have the same definitions except they apply to the perforated panel having a layer of paint or water.

D. Perforated Panel in the Absorber Behind-the-Panel Configuration

For the absorber behind-the-panel configuration shown in Fig. 1(b), let $T_{a,pp,abs}$ and $T_{a',pp,abs}$ be defined as the antenna noise temperatures, respectively, for the

unpainted and painted (or wet) perforated panel test configurations. Then, from Fig. 1(b), it can be seen that

$$T_{a,pp,abs} = A_{pp}[|(S11)_{pp}|^2 T_{sky,zen} + D_{pp}T_p + A_b|(S21)_{pp}|^2 T_p + (1 - A_b)\,|(S21)_{pp}|^2 T_{b,b}] + (1 - A_{pp})\,T_{b,pp} \quad \text{(C-13)}$$

$$T_{a',pp,abs} = A'_{pp}[|(S11')_{pp}|^2 T_{sky,zen} + D'_{pp}T_p + A_b|(S21')_{pp}|^2 T_p + (1 - A_b)\,|(S21')_{pp}|^2 T_{b,b}] + (1 - A'_{pp})\,T_{b,pp} \quad \text{(C-14)}$$

where A_b is the fraction of leakage wave power captured by the absorber and is assumed to be the same value for the above primed and unprimed measurements. Also, $T_{b,b}$ is the average brightness temperature as seen by the portion of perforated panel leakage wave that was not captured by the absorber, K. To account for polarization, it is necessary only to substitute Eqs. (C-9) and (C-10) into Eqs. (C-13), and Eqs. (C-11) and (C-12) into Eq. (C-14).

If the operating noise temperatures for the primed and unprimed cases are differenced, the result is equivalent to subtracting Eq. (C-13) from Eq. (C-14). Then, after the differencing operating is performed, the term involving $T_{sky,zen}$ may be dropped due to making an assumption that it is small compared to the other terms. The result is a noise temperature value that includes both differential panel dissipative loss and leakage loss. If A_b is not equal to unity, a small error term must also be considered. The same comments made for the wet plate case in the horizon sky configuration also apply to this "ambient load" configuration.

E. Perforated Panel in the Solid Plate Behind-the-Panel Configuration

For the solid plate behind-the-panel configuration shown in Fig. 1(c), let $T_{a,pp,sp}$ and $T_{a',pp,sp}$ be defined as the antenna noise temperatures, respectively, for the unpainted and painted (or wet) perforated panel test configurations. Then, from Fig. 1(c), it can be seen that

$$T_{a,pp,sp} = A_{pp}\{|(S11)_{pp}|^2 T_{sky,zen} + D_{pp}T_p + A_c|(S21)_{pp}|^2\,[|(S11)_{sp}|^2 T_{sky,zen} + D_{sp}T_p] + (1 - A_c)\,|(S21)_{pp}|^2 T_{b,c}\} + (1 - A_{pp})\,T_{b,pp} \quad \text{(C-15)}$$

$$T_{a',pp,sp} = A'_{pp}\{|(S11')_{pp}|^2 T_{sky,zen} + D'_{pp}T_p + A_c|(S21')_{pp}|^2\,[|(S11)_{sp}|^2 T_{sky,zen} + D_{sp}T_p] + (1 - A_c)\,|(S21')_{pp}|^2 T_{b,c}\} + (1 - A'_{pp})\,T_{b,pp} \quad \text{(C-16)}$$

where A_c is the fraction of power in the leakage wave captured by the solid plate behind the perforated panel and is assumed to be the same value for the above primed and unprimed measurements. Also, $T_{b,c}$ is the average brightness temperature as seen by the portion of perforated plate leakage signal that was not captured by the solid plate, K. To account for polarization, it is necessary only to substitute Eqs. (C-9) and (C-10) into Eq. (C-15) and Eqs. (C-11) and (C-12) into Eq. (C-16).

For this test configuration, after differencing the antenna noise temperatures for the primed and unprimed cases, the terms involving products with $T_{sky,zen}$ can be dropped. The term $D_{sp}T_p$ may also be dropped. The same comments made for the wet plate case in the horizon sky configuration also apply to this solid-plate configuration.

The presentations of equations for the various test configurations have now been completed. The equations are very useful for error analysis purposes and for developing methodologies for isolating particular noise temperature contributions of interest. It should be mentioned that if the dissipative loss contributions are very small, and it is desirable to determine them very accurately, then the dropping of terms may not be permissible.

F. Applications

An interesting application of the above presented equations is to separate the dissipative loss and leakage loss contributions of the perforated panel.

Subtraction of the operating noise temperatures for the perforated panel in the absorber behind-the-panel configuration and the solid reference plate [from Eqs. (C-1), (C-2), and (C-13)], results in the expression

$$T_{a,pp,abs} - T_{a,sp} = \left[|(S11)_{pp}|^2 - |(S11)_{sp}|^2\right] T_{sky,zen} + (D_{pp} - D_{sp})\,T_p + |(S21)_{pp}|^2\,T_p \quad \text{(C-17)}$$

where it was assumed in Eq. (C-2) that $A_{sp} = 1$ and in Eq. (C-13) $A_{pp} = 1$ and $A_b = 1$. The first, second, and third terms in the above equation, respectively correspond to differential contributions due to reflection, dissipation,

and leakage. If it can be assumed that the first term can be dropped because it is small compared to the other terms, then the remaining terms provide information concerning the contributions due to both dissipation and leakage.

Now, differencing the operating noise temperatures for the perforated panel in the solid-plate behind-the-panel configuration and the solid reference plate [from Eqs. (C-1), (C-2), and (C-15)] results in the expression

$$T_{a,pp,sp} - T_{a,sp} = \left(|(S11)_{pp}|^2 - |(S11)_{sp}|^2\right) T_{sky,zen} + (D_{pp} - D_{sp})\, T_p + |(S21)_{pp}|^2 |(S11)_{sp}|^2 T_{sky,zen} + D_{sp} T_p \tag{C-18}$$

where it has been assumed in Eq. (C-2) that $A_{sp} = 1$ and in Eq. (C-15) that $A_{pp} = 1$ and $A_c = 1$. In Eq. (C-18), if it is assumed that the first and third terms can be dropped, then the results are just the differential dissipative loss noise temperature contribution of the perforated plate.

In order to obtain the leakage wave contribution, one can difference the operating noise temperatures of the perforated panel in the absorber and solid plate behind the panels. Then, performing this differencing through the use of Eqs. (C-1), (C-13), and (C-15), one obtains

$$T_{a,pp,abs} - T_{a,pp,sp} = |(S21)_{pp}|^2 \left[T_p - |(S11)_{sp}|^2 \left(T_{sky,zen} + D_{sp} T_p\right)\right] \tag{C-19a}$$

where it has been assumed that $A_{pp} = 1$, $A_b = 1$, and $A_c = 1$. If we further assume that $|(S11)_{sp}|^2 = 1$ and $D_{sp}T_p$ is small compared to $T_{sky,zen}$, then differencing the operating noise temperatures will result in an approximate leakage wave noise temperature contribution of

$$T_{a,pp,abs} - T_{a,pp,sp} = |(S21)_{pp}|^2 \left(T_p - T_{sky,zen}\right) \tag{C-19b}$$